

# A NEW LIDAR SYSTEM FOR THE DETECTION OF CLOUD AND AEROSOL BACKSCATTER, DEPOLARIZATION, EXTINCTION, AND FLUORESCENCE

Franz Immler<sup>1</sup>, Ingo Beninga<sup>2</sup>, Wilfried Ruhe<sup>2</sup>, Bernhard Stein<sup>3</sup>, Bernd Mielke<sup>3</sup>, Soeren Rutz<sup>3</sup>,  
Özden Terli<sup>1</sup>, Otto Schrems<sup>1</sup>

(1) Alfred Wegener Institute for Polar and Marine Research P.O. 120161, D-27515 Bremerhaven, Germany

E-mail: fimmler@awi-potsdam.de

(2) impres GmbH, Bremen, Germany, E-mail: beninga@impres.hb.uu.net.de

(3) Licel GmbH, Berlin, Germany, E-mail: stein@licel.com

## ABSTRACT:

We present a newly designed **Compact Cloud and Aerosol LIDAR (ComCAL)** that was built for the deployment in field campaigns on ground and on mobile platforms like aboard the research vessel Polarstern. The automated system is particularly suited for tropospheric aerosol research within the altitude range from 0.7 to 20 km. As emitter it uses a frequency doubled and tripled Nd:YAG laser. It measures elastic backscatter and the depolarization at 532 nm and 355 nm as well as inelastic scattering with a 32-channel spectrograph. Recently, it was shown that biomass burning aerosol fluoresces when irradiated by a UV laser beam while other aerosol types do not fluoresce [1]. Beside the detection of N<sub>2</sub> and H<sub>2</sub>O Raman scattering, fluorescence of aerosols can be detected by the new optical set-up of our lidar system. The measurement of wavelengths dependent backscatter, extinction, depolarization, and fluorescence makes a detailed study of atmospheric aerosols possible. The new lidar system deter-

mines optical properties of aerosols and their vertical distribution. The aerosol types, their origins and abundance can be deduced from that data. These are important parameters for the study of the effect of natural and anthropogenic aerosols on the earth's climate.

## 1. INTRODUCTION

Aerosols and clouds have an important impact on the climate of the earth by interfering with the transfer of radiation through the atmosphere. The uncertainties about this impact are rather large due to the large natural variability of aerosol abundance and an insufficient knowledge of the physical processes that are involved in cloud formation [2].

Different types of aerosol have different optical characteristics. The backscatter of dust for example is depolarized due to the non-spherical shape of the particles. Since Saharan dust generally contains iron oxides, it strongly absorbs in the blue and near UV (giving its auburn color). This absorption can be observed by a multi-wavelength lidar that uses i.e. the doubled and tripled harmonic of a Nd:YAG laser. The wavelengths dependence of the backscatter coefficient  $\beta$ , which can be determined from lidar signals is expressed by the color index  $C_i$ :

$$C_i = \frac{-\ln \beta(\lambda_1) - \ln \beta(\lambda_2)}{\ln \lambda_1 - \ln \lambda_2}$$

The absorption properties of Saharan dust yield a negative color index [3]. Black absorbers like soot or non absorbing particles like sulfates have a positive color index with a magnitude which primarily depends on the size of the particles. The smaller the particles, the larger is the color index. The stronger absorption by soot in comparison to sulfate is reflected in a larger extinction-to-backscatter ratio, -or 'lidar ratio' - which is higher for absorbing articles (typically around 60) compared to liquid sulfate aerosol droplets which typically have values around 20. This ratio can be determined by the Raman lidar technique [4].

The measurement of these optical properties of aerosols allow a classification of different types and in the case of spherical particles a retrieval of microphysical properties like size distribution [5]. It was recently shown that aerosols originating from biomass burning fluo-

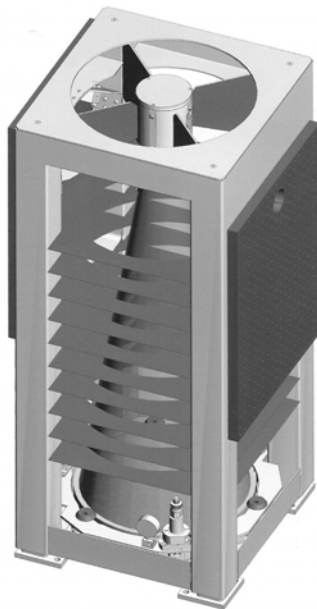


Fig. 1: View of the telescope frame that holds all optical components of the lidar system

resce when irradiated with a UV laser beam [1]. The detection of fluorescence from atmospheric aerosols can be used as an indicator for the presence of different types of organic aerosol particles from natural or anthropogenic sources like biomass-burning or fossil fuel combustion. However, little is so far known about the characteristics and spectra of the laser-induced fluorescence of these different types of aerosols.

In order to investigate the optical properties of aerosols in detail we have constructed a lidar system which measures backscatter at three wavelengths (1064 nm, 532 nm, 355 nm), that uses the Raman technique to determine the extinction, and that is able to measure fluorescence or Raman scattering [6] from particles in the atmosphere.

## 2. MECHANICAL DESIGN OF COMCAL

Our intention was to build a system that can be used in field experiments on ground or on mobile platforms like trucks, trains or ships. Consequently, the design of the lidar system had to meet challenging mechanical specifications. In particular the system was constructed for automatic operation, allowing to leave it unattended while temperature changes, inclination and vibrations occur. Therefore, we chose a design with a telescope in Newtonian configuration with the sending and receiving optics mounted to one rigid frame (Fig. 1). This de-

sign is mechanically very stable and allows a set-up with a minimum of optical components.

The telescope frame is contained in a cabinet and is actively temperature stabilized by heaters and ventilators. A window which is split into an uncoated receiving and a coated sending part is mounted to the housing of the system and closes the stabilized area to the outside. Primary and secondary mirror are adjustable. The sending mirror on top of the secondary mirror is mounted on gimbal axes which are driven by computer controlled stepping motors to permit a computer aided adjustment procedure.

## 3. OPTICAL DESIGN OF THE INSTRUMENT

A Nd:YAG Laser (Quantel Brilliant) emits light pulses at 1064 nm, 532 nm, and 355 nm vertically into the atmosphere with 120 mJ, 180 mJ, and 65 mJ, respectively, and a repetition rate of 20 Hz. The laser beam is expanded to 5 times its original diameter (6 mm) in order to reduce the divergence. Two dielectric mirrors deflect the expanded laser beam to the axis of the receiving telescope (Fig. 2).

The backscattered light from the atmosphere is collected by a parabolic mirror with 400 mm aperture and 1200 mm focal length. A flat secondary mirror directs the received light to a pinhole ( $\varnothing 1$  mm) in a bread-board that holds the detector optics. A 90°-off-axis-

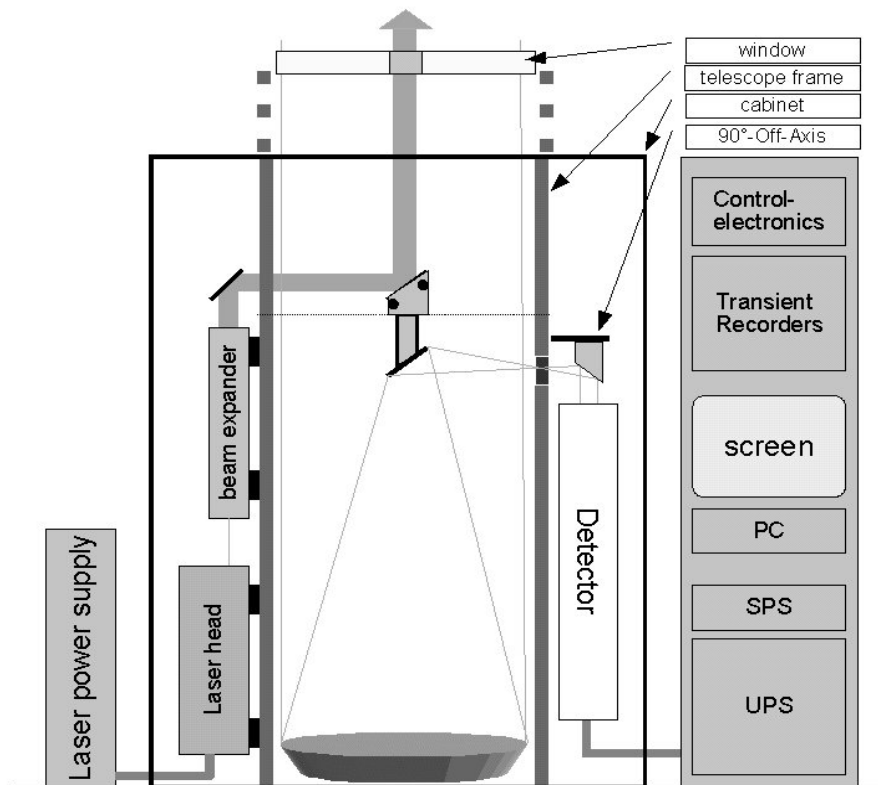


Fig. 2: Schematic diagram of the new ComCAL system.

Table 1: Specifications of the elastic detector channels

channel	Filter: CWL, FWHM, max. Transmission	Detector
1064 nm	1063.8 nm, 2.81 nm, 82%	Licel APD-1.5mm
532 nm	532.08 nm, 0.33 nm, 36%	Hamamatsu H7680-02
355 nm	354.8 nm, 0.98 nm, 52%	Hamamatsu H7680-03

parabolic mirror deflects the light by 90° and simultaneously parallelizes it (Fig. 3). A broadband dichroic mirror separates the elastic and inelastic wavelengths. Light at the wavelengths 355 nm, 532 nm, and 1064 nm is reflected with an efficiency of 99.6%, 99.75%, and 80%, respectively, while light in the range from 370 nm to 490 nm is transmitted by at least 90%. While the light at 1064 nm is directly detected by an Avalanche Photo Diode (APD), the light at the wavelengths of 532 nm and 355 nm passes through a rotating Glan-Taylor prism which is synchronized with the laser (Fig. 4). Thus, the light polarized parallel and perpendicular to the laser's polarization are detected alternately. This configuration allows the measurement of the depolarization without the need for a calibration since the same detection channel is used for both polar-

ization directions. The signals are recorded by Licel transient recorders (20 MHz, 12 bit) in analog and photon counting mode simultaneously.

The inelastic light is coupled into a fibre bundle and transmitted to a Czerny-Turner spectrograph with 125 mm focal length and a holographic grating with 1200 lines/mm. This grating creates a beam with dispersion of 6.2 nm/mm that is focused on a multi-anode-photomultiplier tube with 32-channel which are 0.8 mm wide and separated by 0.2 mm. Thus, a spectrum in the range from 370 nm to 430 nm is measured with a resolution of 6.2 nm. A multi-channel photon counting scaler with a 30 m range resolution is currently developed. The Raman signals from nitrogen, oxygen, and water vapor are the dominant features on some of this channels while in the others the fluorescence from organic particles and Raman scattering from liquid water droplets or ice particles are detected.

#### 4. FIRST RESULTS

The new ComCAL Lidar system was first operated during a cruise with the research vessel Polarstern (expedition ANT XXIII/1) from Bremerhaven (Germany) to Cape Town (South Africa) from 13.10.2005 to 17.11.2005.

Elastic scattering was measured during day and night time with a range from 0.5 to at least 15 km. Fig. 5 shows a time series of the backscatter ratio at 532 nm as an example. In the boundary layer sea salt aerosol was detected which was clearly turbulent during the

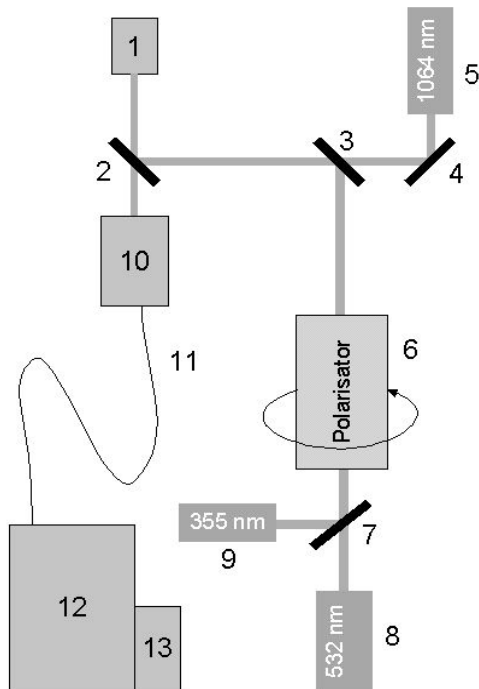


Fig. 3: Schematic diagram of the detector optics: 1: 90° Off-Axis mirror, 2,3,4,7: dichroic mirrors, 5: Detector for 1064 nm Signal (Interference filter, lens, APD), 6: rotating Glan-Taylor prism, 8,9: Detectors for 532 nm and 355 nm signals (Interference Filters, Lens, PMT), 10: Fiber coupler, 11: fibre bundle, 12: Czerny-Turner Spectrograph, 13: Multi-Anode-PMT



Fig. 4: The rotating polarizator unit

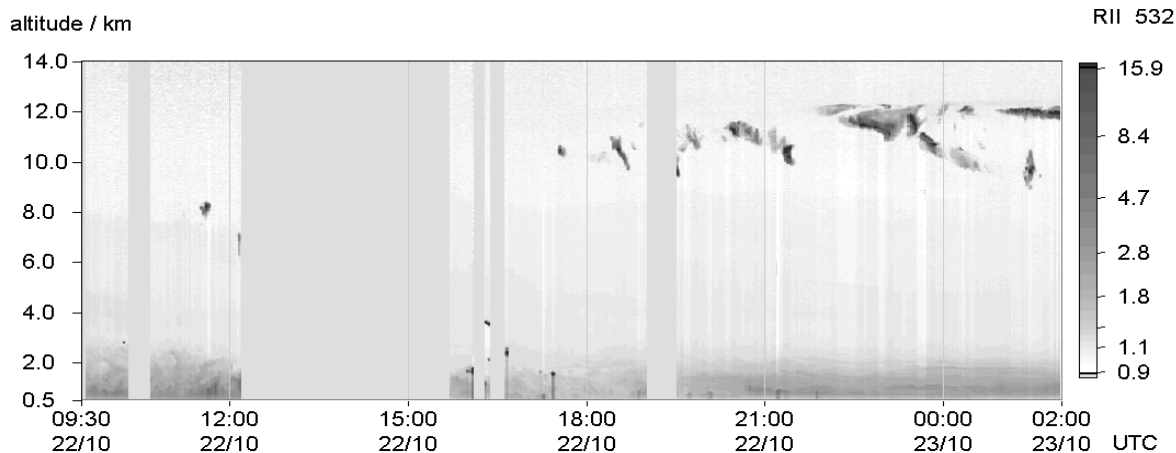


Fig. 5: Time series of the backscatter ratio measured with the ComCAL system aboard FS Polarstern during the cruise ANT XXIII/I on 22 October 2005 in the Atlantic off the west coast of Spain.

day and stratified at night time. Between 10 km and 12 km altitude some scattered cirrus were detected.

In the cloud and aerosol free region the depolarization ratio determined by the ratio of the alternately measured perpendicular and the parallel backscatter without further calibration was  $0.013 \pm 0.005$  and  $0.012 \pm 0.002$  at 355 nm and 532 nm, respectively. These values are explained by the molecular depolarization of the Cabannes line of 0.004 [7] (the purely rotational bands are to a large extent cut off by the narrowband filters) and some intrinsic depolarization of the sending and receiving optics. The intrinsic depolarization is with about 0.8 % at both wavelengths low enough to be neglected for depolarization measurements of clouds and aerosol which is generally 10% or larger.

During the cruise, Saharan dust, sea salt, and biomass burning aerosols were observed in the free troposphere and identified by their optical properties, namely their depolarization and color index. Fig. 6 shows a scatter

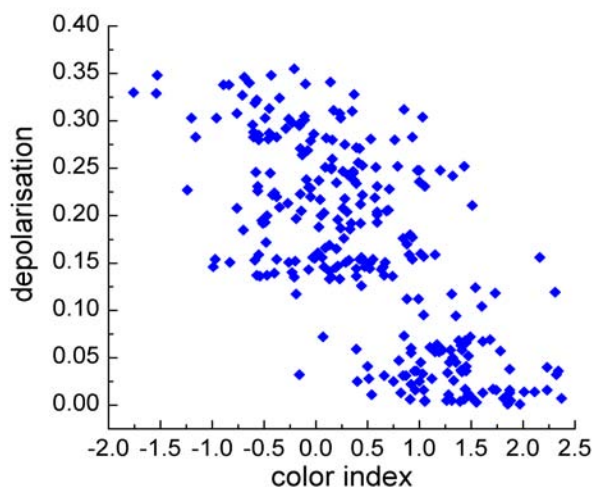


Fig. 6: Color index versus depolarization of free tropospheric aerosol layers measured by ComCAL system during the Polarstern campaign ANT XXIII/I

plot of these two variables. The Saharan dust is identified by large depolarization and a negative color index. The aerosol with low depolarization is a biomass burning plume detected south of the equator, where polluted air masses are advected across the Atlantic from the biomass burning areas of southern Africa. In addition, extremely thin tropical cirrus with optical depths below  $10^{-4}$  have been observed close to the ITCZ at about  $8^{\circ}\text{N}$ .

## 5. SUMMARY

A new lidar system was designed and constructed for cloud and aerosol research in the troposphere. The compact and rugged system measures aerosol backscatter, extinction, depolarization, color index, and fluorescence and thereby allows a classification of different aerosol types. The system was successfully deployed in a ship campaign in 2005. Different types of aerosol were detected and identified.

## 6. REFERENCES

1. Immler F., D. Engelbart, O. Schrems, Atmos. Chem. Phys., 5, 345-355, 2005.
2. International Panel on Climate Change (IPCC), Cambridge University press, Cambridge, 2001.
3. Immler F., O. Schrems, Atmos. Chem. Phys., 3, 1353-1364, 2003.
4. Ansmann A., M. Riesbel, C. Weitkamp, Opt. Lett, 15, 746-748, 1990
5. Wandinger U., et al., J. Geophys. Res., 107, D21, 8125, 2002.
6. Melfi S. H. , K.D. Evans, J. Li, D. Whiteman, R. Ferrare, G. Schwemmer , Appl. Opt., 36, 3551-3559, 1997.
7. Behrendt A., T. Nakamura, Optics express, 10, 16, 805-817, 2002.